

A DEVICE FOR MEASURING HEAT TRANSFER
RATES IN ARC-DISCHARGE HYPERVELOCITY
WIND TUNNELS

By
R. L. Ledford
von Kármán Gas Dynamics Facility
ARO, Inc.
a subsidiary of Sverdrup and Parcel, Inc.

May 1962
ARO Project No. 366920

Contrails

ABSTRACT

Heat-transfer-rate is one of the fundamental aerodynamic parameters which must be measured in Hypervelocity wind tunnel testing. Transducers which can perform this measurement are not commercially available; therefore a device which can be employed for this purpose has been developed. This device can measure transient rates ranging from 1 to 1000 Btu/ft² sec for periods of 5 to 80 millisecc; it does not require run-to-run calibration; and it is durable enough to withstand many tunnel runs without maintenance. Its performance has been proven through laboratory and tunnel tests and usage.

Contrails

CONTENTS

	<u>Page</u>
ABSTRACT	iii
NOMENCLATURE	vii
1.0 INTRODUCTION	1
2.0 TRANSDUCER DESCRIPTION AND THEORY OF OPERATION	
2.1 TCG Sensitivity	2
2.2 Experimental Calibrations	3
2.3 TCG Selection	4
2.4 TCG Frequency Response	5
3.0 INSTRUMENTATION	
3.1 Differentiator Readout	8
3.2 Differentiator Evaluation	10
4.0 PERFORMANCE AT TEST CONDITIONS	11
5.0 CONCLUSIONS	12

ILLUSTRATIONS

Figure

1. Thermocouple Heat Transfer Gage	13
2. Comparison of Calibrated Heat Input and Heat-Transfer-Rate Indicated by TCG When Employing Theoretical TCG Sensitivity	14
3. TCG Output versus Time with Oxyacetylene Torch Heat Input	15
4. Heat-Transfer-Rate versus TCG Copper Disk Temperature	16
5. Transfer Function for a Semi-Infinite Slab	17
6. Slab Thickness versus Frequency	18
7. Instrumentation System for Heat Transfer Measurement with Thermocouple Gage (TCG).	19
8. Heat Transfer Instrumentation System Employing Differentiator	20
9. Differentiator Circuit	21
10. Transfer Function of Differentiator and Galvanometer	22

<u>Figure</u>	<u>Page</u>
11. Phase Shift of Differentiator and Galvanometer. . .	23
12. Comparison of Torch and Differentiator Heat Transfer Data	24
13. Typical Oscillographic Trace of Linear and Differentiated TCG Output	25
14. Comparison of Slope and Differentiated Heat Transfer Data	26
15. Three-Inch Hemisphere Cylinder Heat Transfer Model	27
16. Hotshot Oscillographic Data Trace	28
17. Comparison between Theoretical and Experimental Heat Transfer Rates versus S/r	29

NOMENCLATURE

A	Area, in. ²
C	Capacitance, farad
c _p	Specific heat, $\frac{\text{Btu}}{\text{lb}^\circ\text{F}}$
e	Electromotive force, volt
f	Frequency, cps
h	Film coefficient, $\frac{\text{Btu}}{\text{ft}^2\text{sec}^\circ\text{R}}$
i	$\sqrt{-1}$
K	$\left(\frac{\omega}{2\alpha}\right)^{1/2}$
k	Thermocouple gage constant, $\frac{\text{millivolt/sec}}{\text{Btu/ft}^2\text{sec}}$
l	Slab or disk thickness, in.
m	Mass, lb
N	Amplifier attenuation
Q	Heat, Btu
\dot{q}	$\frac{dQ}{dt}$, $\frac{\text{Btu}}{\text{ft}^2\text{-sec}}$
R	Resistance, ohm
r	Radius, in.
S	Surface distance from stagnation point of model, in.
T	Temperature, °R
T.F.	Transfer Function
T _D	Disk temperature, °R
T _F	Flame temperature, °R
t	Time, sec
V	Volume, in. ³
x	Slab or disk depth measured from the back surface, in.
α	Thermal diffusivity, in. ² /sec

β	Constant
γ	Constant
δ	Galvanometer deflection, in.
ϵ	Naperian base, 2.718
μ	Damping ratio
π	3.1416
ρ	Density, lb/in. ³
ω	Frequency, rad/sec
ϕ	Phase angle, deg

SUBSCRIPTS

o	Out
in	In
N	Natural
RC	Resistance-capacitance
cal	Calibration
s	Stagnation point

1.0 INTRODUCTION

Transient heat transfer rates ranging upward to approximately 1000 Btu/ft² sec are produced in the intermittent, electric, arc-driven (Hotshot) wind tunnels of the von Kármán Gas Dynamics Facility (VKF), Arnold Engineering Development Center (AEDC), Air Force Systems Command (AFSC). The run duration of these tunnels is from 20 to 80 milliseconds.

A heat-transfer-rate transducer, which may be employed to measure these transient heat-transfer-rates, has been developed by the VKF Instrumentation Branch. This transducer utilizes a copper disk as a calorimetric mass and a thermocouple as a temperature sensor. It is presently used for all heat-transfer-rate measurements in the VKF Hypervelocity wind tunnels. A detailed description of this transducer and its associated instrumentation is given in this report along with the results of an evaluation test conducted on the entire system.

2.0 TRANSDUCER DESCRIPTION AND THEORY OF OPERATION

The thermocouple heat-transfer-rate transducer, hereafter referred to as the TCG, is shown in Fig. 1. It is ordinarily installed in the wall of a test model; it can be fabricated with flat or contoured calorimeter disks so that its outer surface will be flush with the model exterior. The transducer's external dimensions are approximately 0.250-in. -diam by 0.312 in. long. Coaxial, or two-conductor-shielded, electrical leads are employed to ensure a minimum amount of noise pickup.

The theory of operation of the TCG is that of a calorimeter; a copper disk of uniform thickness serves as the calorimetric mass; and a thermocouple is employed as the temperature sensor. The copper disk is cemented into a nylon bushing so that one side of the disk is exposed to the tunnel flow when the transducer is mounted in a model. The nylon bushing insulates the copper disk so that little heat is lost from it during the tunnel run. A thermocouple senses the disk's temperature. The thermocouple wires are resistance-welded or swaged onto the disk. Chromel-constantan wires are most frequently used for the thermoelements; this pair was selected for its high output and its low thermal conductivity. The size of the wires employed ranges from 0.0005 to 0.0020-in. diam,

Manuscript released by author April 1962.

depending on the thickness of the copper disk with which they are used. The wires must be of such a size that they conduct a negligible amount of heat away from the disk.

2.1 TCG SENSITIVITY

The sensitivity of the transducer may be computed if the following conditions are met:

1. The copper disk thickness is uniform and can be measured accurately.
2. The density and specific heat of the copper disk are known and are constant throughout the temperature range to which the disk will be subjected.
3. The thermoelectric output of the thermoelements is known and approximately linear.
4. The temperature gradient through the copper disk is negligible.
5. All heat is added through the front surface of the disk, and no heat is lost from the disk.

It has been experimentally verified that the transducer can be constructed in such a fashion that all these conditions can be met within acceptable limits. Methods by which these respective conditions listed can be met are as follows:

1. Precision-rolled copper is employed for disk material.
2. The temperature rise of the copper disk is kept below 250 to 300°F while heat-transfer-rate measurements are being made; therefore density and specific heat are practically constant.
3. Thermoelements with an output curve which is very nearly linear for a 250 to 300°F rise above room temperature are used.
4. The thickness of the copper disk used is such that there is a negligible temperature gradient through the disk.
5. The disk is mounted so that it is well insulated (thermally) with the exception of its front surface which will be exposed to the heat input which is to be measured.

To compute the transducer sensitivity, consider that the quantity of heat contained by anybody is given by the expression:

$$Q = mc_p T$$

The rate of heat transfer into the body is likewise given by:

$$\dot{q} = \frac{1}{A} \frac{dQ}{dt}$$

$$\therefore \dot{q} = \frac{m c_p}{A} \frac{dT}{dt}$$

$$m = \rho V$$

For a disk: $V = \pi r^2 \ell$ and $A = \pi r^2$

Substituting:

$$\dot{q} = \rho \ell c_p \frac{dT}{dt}$$

$$de = \gamma dT$$

$$\therefore \dot{q} = \frac{\rho \ell c_p}{\gamma} \frac{de}{dt}$$

It is seen that the heat-transfer-rate may be determined by recording the temperature rise of the copper disk with respect to time; i. e., the slope of the time-resolved output of the transducer is proportional to heat-transfer-rate. Instantaneous heat rates are directly proportional to the time derivative of temperature. The sensitivity of the transducer is:

$$\frac{\frac{de}{dt}}{\dot{q}} = \frac{\gamma}{\rho \ell c_p}$$

As can be seen from this equation, the sensitivity of the transducer is dependent only upon the thickness of the copper disk for a given thermo-element.

2.2 EXPERIMENTAL CALIBRATIONS

Experimental calibrations, which have been made with oxyacetylene torches, have produced sensitivity values which are generally within 10 percent of those sensitivities which are computed. Figure 2 shows the heat-transfer-rate indicated by a TCG, as computed from the transducer's theoretical sensitivity, when it is subjected to a known heat input from an oxyacetylene calibration torch.¹ Data points from several transducers at

¹Morgan, C. C. and Andrews, J. C. "Morgandyne Heat-Transfer Transducer and a Flame-Torch Calibration Technique for Hypervelocity Wind Tunnels." AEDC-TR-60-1, February 1960.

different heat-transfer-rates are shown. The small scatter which is exhibited by these typical data points has resulted in the adoption of the computed sensitivities as the values which are employed in the reduction of test heat transfer data. However, each new transducer is checked with the calibration torch before it is put into service to ensure that it functions properly.

2.3 TCG SELECTION

In the selection of a TCG for making a given heat-transfer-rate measurement, one basic factor must be considered, i. e., the temperature rise of the calorimetric mass during the tunnel run. The temperature rise is dependent on the following factors; the heat rate which is to be measured, the duration of the run, and the copper disk thickness.

Certain limitations which determine what the temperature rise of the disk may be in order that the TCG function properly are:

1. The temperature rise of the disk must not exceed the working limits of the cement which is used to hold the copper disk in the nylon insulator.
2. The temperature rise must be small enough to prevent an intolerable heat loss from the disk.
3. The temperature rise must be sufficiently large to produce an electrical signal from the thermoelement which can be recorded accurately.

It is apparent that a compromise must be made. A value of 250 to 300°F has been selected as the permissible temperature rise for the present TCG design. This value was chosen after experimental tests were made to determine the maximum allowable temperature rise.

These tests were made in the following manner: the flame of an oxyacetylene torch was directed onto a gage and held there for 250 to 1000 milliseconds. During this time, the temperature rise of the disk was recorded on an oscillograph. A typical trace is shown in Fig. 3. Ideally, the curve shown in the figure would be a straight line of constant slope; however, as time (and thus temperature of the disk) increases, the heat losses from the disk increase. Eventually equilibrium could be reached (the heat losses from the disk would equal the heat input and the disk temperature would stabilize at a constant value) if the transducer could withstand the heat input of the torch for a sufficiently long period of time without failure.

To determine what temperature rise can be tolerated, the temperature rise beyond which the slope of the curve (de/dt) deviates from the theoretical slope by an intolerable percentage is established. The allowable temperature rise varies for transducers whose nominal disk thicknesses are not the same; however, a rise of approximately 250°F will not produce an error greater than 2 percent for transducers whose disks range from 0.005 to 0.020 in. thick (when they are used at nominal stagnation temperature of 3000°K).

A unique feature of the TCG permits the entire deviation of the slope of the temperature versus time curve in these tests to be attributed to heat losses from the disk. This is that the nonlinearity of the chromel-constantan thermocouple, which is used to sense the disk temperature, is in such a direction and of such a magnitude that it compensates to a large extent for the decrease in convective heat-transfer-rate (because of the increase in disk temperature) from the torch to the disk. This can best be explained by reference to Fig. 4. As can be seen from this figure, the indicated heat-transfer-rate from a TCG which has no losses and which is exposed to a constant heat input rate would be as shown by curve A. Curve B represents the decay in convective heat-transfer-rate from an oxyacetylene torch with a flame temperature of approximately 6000°F. The equation for this curve is:

$$\dot{q} = h(T_F - T_D)$$

(Previous work has shown that the heat transferred from an oxyacetylene torch is largely convective.) The mean of curves A and B is shown by curve C, and it is seen that the error remains small for temperature rises below 300°F. Therefore it is apparent that the nonlinearity of the heat rate from an oxyacetylene torch compensates, to a great extent, for the nonlinearity of the chromel-constantan sensor in a TCG.

Fortunately, most Hotshot tunnel tests in the VKF are presently made with nominal stagnation temperatures of 3500°K (6300°F) which is very near the calibration-torch flame temperature. This means that the aforementioned compensating effect is present during a tunnel run. Runs with nominal stagnation temperatures above and below the standard 3500°K can produce errors accruing from the summation of the thermocouple nonlinearity and the convective heat-transfer-rate decay; however, with disk temperature rises of 250°F or less this error can never exceed 5 percent for stagnation temperatures greater than 1650°K.

2.4 TCG FREQUENCY RESPONSE

Transducers with disk thicknesses ranging from 0.002 to 0.020 in. have been employed for tunnel measurements ranging from 2 to 1000 Btu/ft²sec.

The response of transducers with these disk thicknesses has been shown experimentally and analytically to be adequate for Hotshot measurements.

An analysis of the ratio of the back surface to the average temperature of an infinite slab when subjected to a sinusoidally varying heat flux gives one an idea of the response of the TCG copper sensing disk. To apply this analysis to the TCG, the following assumptions must be made:

1. Heat losses from the back and edges of the sensing disk are negligible.
2. Heat is added to the disk only through the front surface.
3. The heat flux is uniform over the front surface.
4. The thermal diffusivity of the disk is constant.
5. The thermocouple senses the back surface temperature of the disk.

The actual heat-transfer-rate of the TCG (\dot{q}_{actual}) is proportional to the time derivative of the average disk temperature (T_{average}). The indicated or measured heat-transfer-rate ($\dot{q}_{\text{measured}}$) is proportional to the time derivative of the back surface temperature (T_{back}). The transfer function from a heat transfer standpoint is therefore:

$$\text{T.F.} = \frac{dT_{\text{back}}}{dT_{\text{average}}}$$

From Carslaw and Jaeger's "Conduction of Heat in Solids," the temperature distribution in an infinite slab with a sinusoidal front surface temperature is:

$$dT_x = \frac{\cosh Kx(1+i)}{\cosh Kl(1+i)} dT_{\text{front surface}}$$

where
$$K = \left(\frac{\omega}{2\alpha}\right)^{1/2} = \left(\frac{\pi f}{\alpha}\right)^{1/2}$$

and
$$dT_{\text{front surface}} = dT_0 \epsilon^{i\omega t}$$

$$\text{T.F.} = \frac{dT_{\text{back}}}{dT_{\text{average}}} = \frac{dT_0 \epsilon^{i\omega t} \left[\frac{1}{\cosh Kl(1+i)} \right]}{\int_0^l dT_0 \epsilon^{i\omega t} \left[\frac{\cosh Kx(1+i)}{\cosh Kl(1+i)} \right] dx}$$

$$= \frac{Kl(1+i)}{\sinh Kl \cos Kl + i \cosh Kl \sin Kl}$$

$$\left| \frac{dT_{\text{back}}}{dT_{\text{average}}} \right| = \frac{Kl \sqrt{2}}{\sqrt{\sin^2 Kl + \sinh^2 Kl}}$$

The phase angle or lag between dT_{back} and dT_{average} is given by:

$$\phi = \tan^{-1} \left[- \frac{\cosh K\ell \sin K\ell - \sinh K\ell \cos K\ell}{\cosh K\ell \sin K\ell + \sinh K\ell \cos K\ell} \right]$$

Figure 5 is a plot of $|dT_{\text{back}}/dT_{\text{average}}|$ and ϕ versus f/f_0 , where f_0 is defined as f when $K\ell = 1$. A plot of f_0 versus ℓ , using the diffusivity of copper and silver, is shown in Fig. 6.

From Figs. 5 and 6, the response of the TCG to sinusoidal heat inputs may be determined. For copper disk thicknesses of 0.020 in. and less, the response of the TCG is seen to be flat within 10 percent for all frequencies below approximately 320 cycles per second; the response increases with decreasing disk thickness.

3.0 INSTRUMENTATION

The output from the TCG appears as an analog voltage which is proportional to the disk temperature. The slope of the time-resolved-output of the transducer is proportional to heat-transfer-rate. A typical sensitivity value is 0.8 mv/sec/Btu/ft²sec. Thus, for a rate of 50 Btu/ft²sec and a run time of 25 milliseconds, the maximum output of the TCG would be one millivolt. Since the TCG requires a time-resolved record of its temperature rise to permit acquisition of heat-transfer-rate data, an oscillograph may be employed as the recording device. One millivolt is too small a voltage to record directly on a galvanometer whose frequency is sufficiently high for Hotshot data; therefore, some means of signal amplification must be employed.

Two devices have been employed for amplification of the TCG signal: d-c amplifiers, and carrier amplifier-demodulators with chopper input circuitry. The operation and hook-up of d-c amplifiers is rather straightforward and well known; however, the operation of the chopper input circuitry which is employed with a carrier system is not as well known. Therefore, a description of the elements and operating characteristics peculiar to this system seems appropriate.

The circuit diagram is shown in Fig. 7. A commercially available transistorized chopper which acts as a SPDT switch is connected through the circuitry shown to a 20-kc carrier amplifier. The drive voltage for the chopper is obtained from the amplifier through the attenuating network. A ferrite core transformer, with a grounded shield between the primary and secondary windings, is used to couple the output of the chopper circuit to the amplifier. This transformer-chopper combination gives an approximate 3 to 1 step-up in signal voltage, thereby giving additional system sensitivity.

The operation of the system is as follows:

1. The analog voltage from the TCG is used to amplitude modulate the 20-kc carrier.
2. The carrier-amplifier system amplifies and phase-demodulates the amplitude-modulated signal.
3. The demodulated signal drives the recording galvanometer.

The Hotshot tunnels present unusual electrical noise problems, therefore careful attention has been given to the noise rejection characteristics of the circuit. At frequencies below 200 cps, the common mode rejection ratio has been measured as being better than one million to one (120 db). The self-generated noise level of the circuit is approximately one microvolt. These readout systems have been frequently calibrated at one-half millivolt d-c input signal for one-inch deflection of the galvanometer trace with little or no difficulty arising from noise.

Because of the lower noise susceptibility and greater sensitivity of the chopper input circuitry, plus the fact that carrier instrumentation is already on hand, this type of amplification system is being used at the AEDC with the TCG.

3.1 DIFFERENTIATOR READOUT

Since heat transfer rate is proportional to the time derivative of the transducer output, it is possible to obtain a signal which is directly proportional to heat-transfer-rate if the transducer signal is differentiated. This makes data reduction a simpler and more accurate process since amplitudes can be read with greater ease and accuracy than can slopes.

A passive, analog, differentiating circuit has been developed for the above mentioned purpose. It is a simple R-C circuit and is shown schematically in Fig. 8 which also shows the other system components in block form. As can be seen by this figure there is provision within this circuit for recording both the differentiated and the undifferentiated heat-transfer-rate signal. This permits conventional records to be made simultaneously with differential records for evaluation purposes during tunnel tests.

The transfer function for the differentiator is the combined transfer functions of both the R-C network and the recording galvanometer.

For the R-C network of Fig. 9:

$$T.F._{RC} = \frac{e_o}{e_{in}} = B \left[\frac{1}{1 - \frac{i}{\omega R_T C}} \right]$$

$$B = \left(\frac{R_L}{R_L + R_C} \right) \left[\frac{R_D R_G}{(R_D R_G) R_T} \right]$$

$$R_T = R_S + \frac{R_C R_L}{R_C + R_L} + \frac{R_D R_G}{R_D + R_G}$$

The transfer function for the galvanometer is (Theory of Recording Galvanometers; M. A. LeGette, Consolidated Electrodynamics Corporation):

$$T.F._{galvanometer} = \frac{1}{1 - \left(\frac{f}{f_N}\right)^2 + 2i\mu \left(\frac{f}{f_N}\right)}$$

Figures 10 and 11 show plots of the combined absolute values of the transfer functions and the phase shifts (ϕ), respectively. Theoretical, measured, and ideal plots are shown.

3.1.1 Calibration of Differentiator

Over the frequency range that the circuit performs as a true differentiator;

$$e_o = \beta \frac{d e_{in}}{dt} \quad (\text{time domain})$$

or when

$$e_{in} = e^{i\omega t}$$

$$e_o = \beta i \omega e_{in} \quad (\text{frequency domain})$$

A galvanometer deflection is of interest rather than e_o , and if the amplifier attenuation is to be included in the calibration, the following equations apply:

$$\delta = \frac{\beta}{N} \frac{d e_{in}}{dt}$$

or

$$\delta = \frac{\beta}{N} i \omega e_{in}$$

The constant β can be determined by either:

1. Applying a signal of known $\frac{d e_{in}}{dt}$
2. Applying a sinusoidal signal of known frequency (ω) and amplitude (e_{in}).

The second method has been adopted for two reasons:

1. Ease of obtaining such a signal as compared to a constant $\frac{de_{in}}{dt}$ signal.
2. The signal can be continuous rather than intermittent, thus allowing plenty of time for adjustment of gain.

Using the absolute value of δ and solving for β gives:

$$\beta = \left[\frac{|\delta| N}{\omega e_{in}} \right]_{\text{calibration}}$$

substituting and rearranging gives the test sensitivity:

$$\frac{\delta}{\frac{de}{dt}} = \left[\frac{N_{\text{calibration}}}{N_{\text{run}}} \right] \left[\frac{|\delta|}{\omega e_{in}} \right]_{\text{calibration}}$$

For the thermocouple gage:

$$\dot{q} = \frac{1}{k} \frac{de}{dt} \quad \text{or} \quad \dot{q} k = \frac{de}{dt}$$

Substituting,
$$\delta = \left[\frac{N_{\text{calibration}}}{N_{\text{run}}} \right] \left[\frac{|\delta|}{\omega e_{in}} \right]_{\text{calibration}} (k \dot{q})$$

and
$$\frac{\dot{q}}{\delta} = \left[\frac{N_{\text{run}}}{N_{\text{calibration}}} \right] \left[\frac{\omega e_{in}}{|\delta|} \right]_{\text{calibration}} \left(\frac{1}{k} \right)$$

3.2 DIFFERENTIATOR EVALUATION

The differentiator was first checked in the laboratory by experimentally determining T, F, and ϕ . See Figs. 10 and 11.

Further laboratory evaluation consisted of applying the calibration torch at a known heat-transfer-rate as mentioned in Section 2.2, to a thermocouple heat transfer gage and comparing the torch heat-transfer-rate with the rate indicated by the output of the differentiator (the differentiator was calibrated using the technique previously described). These data are shown in Fig. 12.

To evaluate the differentiator during tunnel testing, the circuit of Fig. 8 was employed for heat-transfer-rate measurements during a series of tests in Hotshot 1. This provided conventional slope traces as well as differentiated traces for each heat-transfer-rate measurement. Figure 13 shows a typical run trace. A total of 230 data points were taken and compared. A plot of the data comparison is shown in Fig. 14.

The comparisons of \dot{q}_{slope} with \dot{q}_{diff} in Fig. 14 show, on that particular test, that the differentiator tends to give results approximately 5 percent higher than the slope data. The direction of this difference could be predicted; since the phase shift (ϕ) data in Fig. 11 show that the differentiator circuit output lags that of an ideal differentiator, and the heat-transfer-rate decayed with time.

Based on both the tunnel and laboratory data, the differentiator performance has been deemed satisfactory, since the indicated errors are small as compared to the present disagreement of $\dot{q}_{\text{measured}}$ and \dot{q}_{theory} .

4.0 PERFORMANCE AT TEST CONDITIONS

Twenty-nine runs were made in Tunnel Hotshot 1 to evaluate the performance of the TCG under test conditions. A three-inch-diameter, hemisphere-cylinder was instrumented with TCG's and pressure transducers as shown in Fig. 15. Both d-c amplifiers and chopper input circuitry were employed during the tests with most runs being made with the chopper inputs, because of their greater sensitivity and lower noise susceptibility. (All data taken were slope data as this series of tests was made before the differentiator was developed.) The primary purpose of these tests was to determine the quality of the heat-transfer-rate data which is obtainable with TCG's used without the benefit of experimental calibration during the tunnel entry. Secondary objectives were to determine whether rates as low as 1-10 Btu/ft²sec could be measured and whether transducers of different sensitivities (different disk thicknesses) agreed when exposed to substantially the same heat rates.

An experimental calibration was performed before the test began to determine whether the gage sensitivities agreed with theory; no other heat transfer calibration was performed during the test.

Oscillograms of typical heat-transfer-rate data traces are shown in Fig. 16. Eighty-two percent of the data taken from symmetrically opposed gages agreed within ± 10 percent. Rates as low as 2 Btu/ft²sec were successfully measured on the cylindrical portion of the model. A graph showing the agreement of typical measured rates with theoretical values is shown in Fig. 17. The discrepancies between $\dot{q}_{\text{measured}}$ and \dot{q}_{theory} are rather large in some instances; however, the ratios of $\dot{q}_{\text{measured}}/\dot{q}_{\text{theory}}$ are fairly constant for any given run at all values of S/r . This indicates that the theoretical heat-transfer-rates may be in error rather than the measured rates.

In another test, a probe which contained five TCG's which were located on stagnation points, was employed in the 50-Inch Hypervelocity Tunnel (Hotshot 2) for 45 consecutive shots during which no calibration of the TCG's was made. At the conclusion of this series of tests, these gages were calibrated with an oxyacetylene torch; it was found that the maximum deviation of any gage from its computed sensitivity was 2.5 percent.

5.0 CONCLUSIONS

Both laboratory and tunnel tests have shown that the TCG can be employed to measure a wide range of heat-transfer-rates in "Hotshot-type" wind tunnels. It has been shown theoretically and experimentally that the TCG's sensitivity can be computed, thus eliminating the necessity of experimental calibrations. The stability of the TCG's sensitivity permits its use without run-to-run calibrations, and the gage is rugged enough to withstand many tunnel runs with little maintenance.

Either d-c amplifiers or carrier-amplifier instrumentation may be used with the TCG, and differentiation techniques can be employed to provide a signal whose amplitude is directly proportional to heat-transfer-rate.

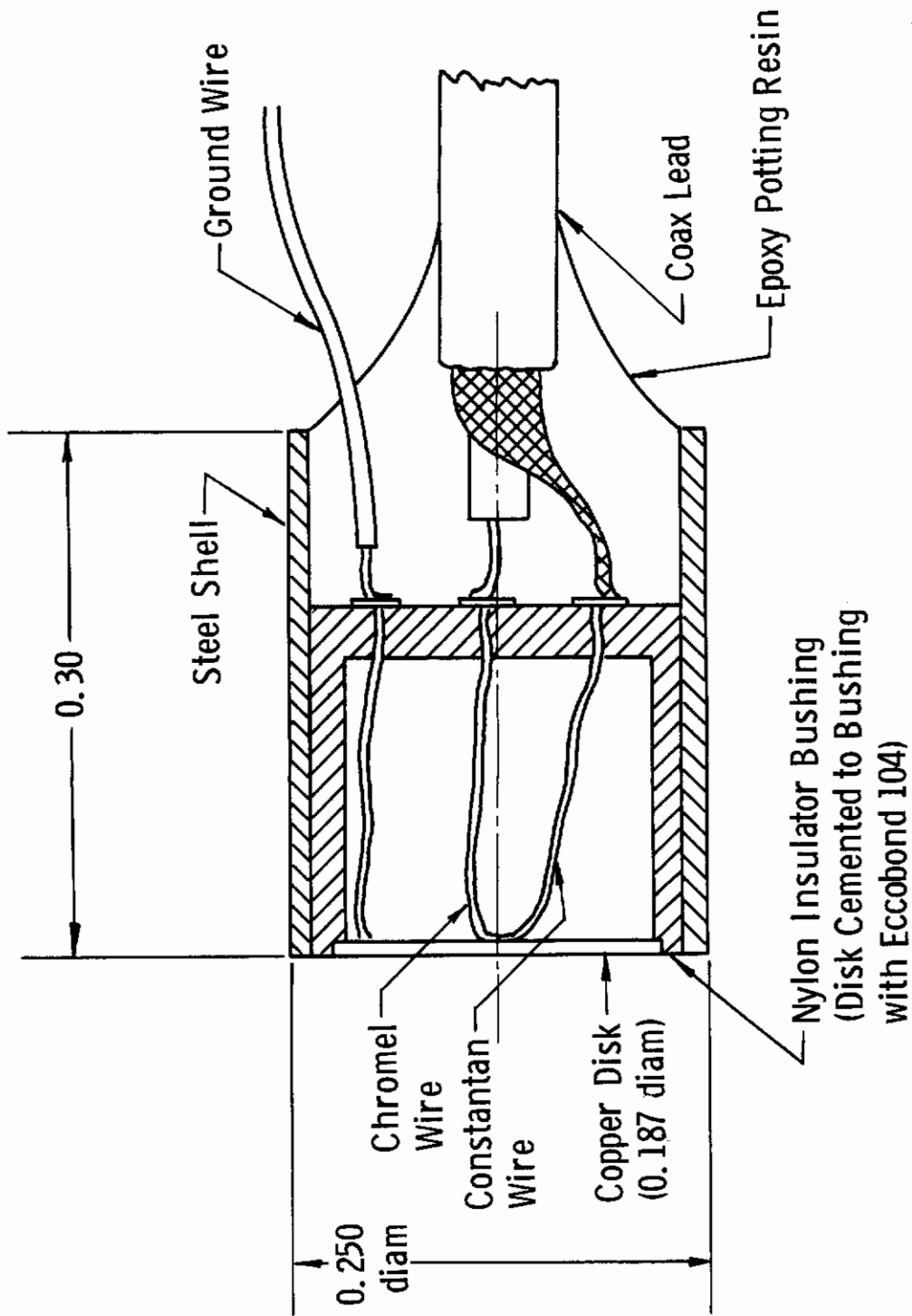


Fig. 1 Thermocouple Heat Transfer Gage

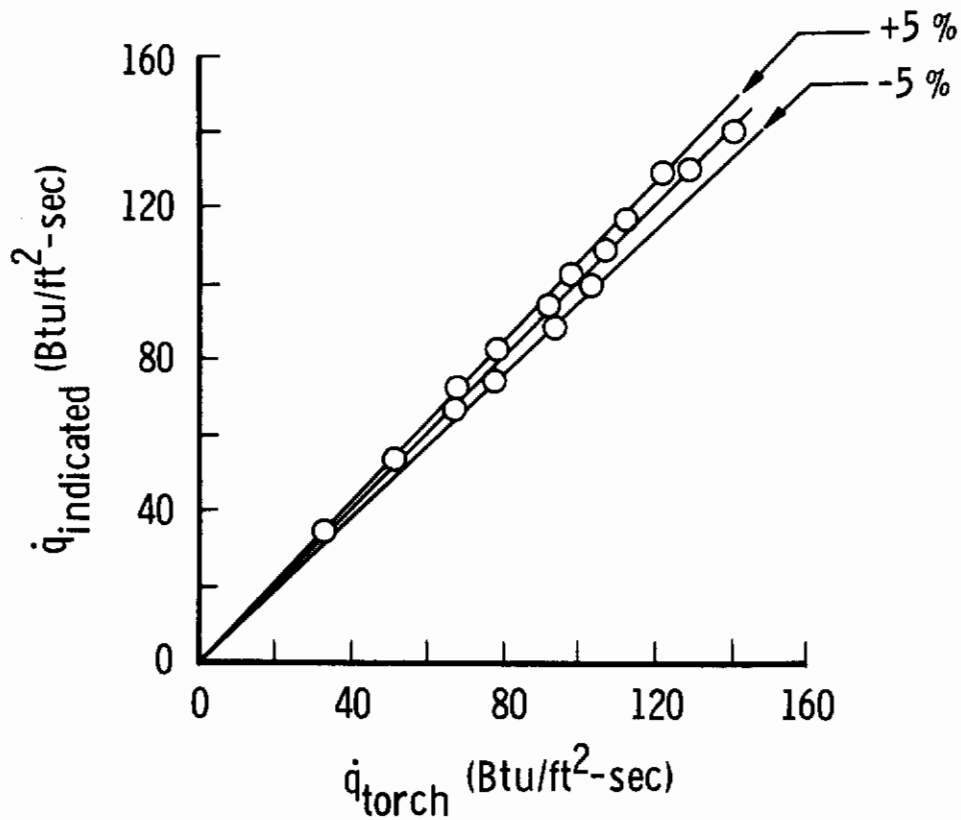


Fig. 2 Comparison of Calibrated Heat Input and Heat-Transfer-Rate Indicated by TCG When Employing Theoretical TCG Sensitivity

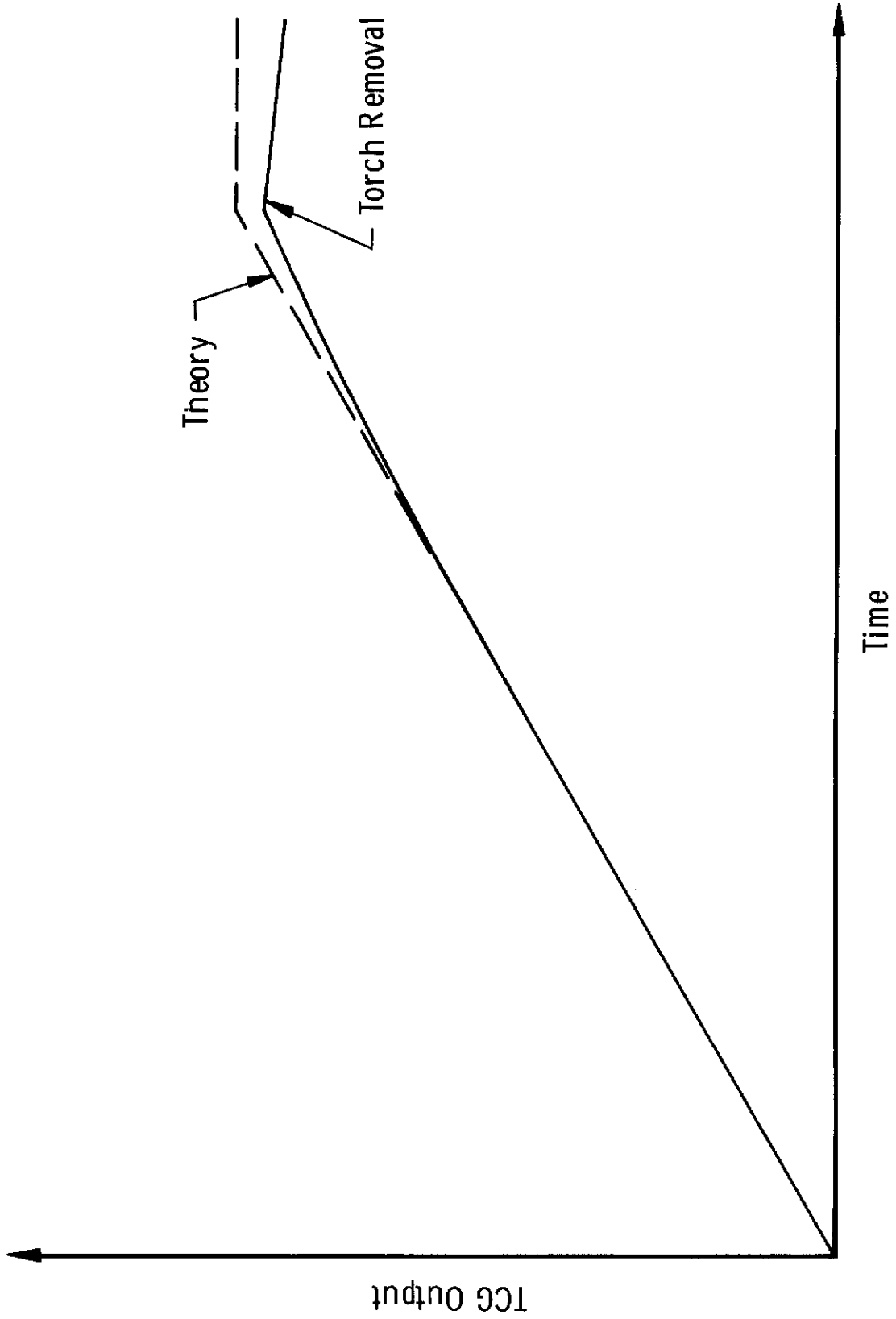


Fig. 3 TCG Output versus Time with Oxycetylene Torch Heat Input

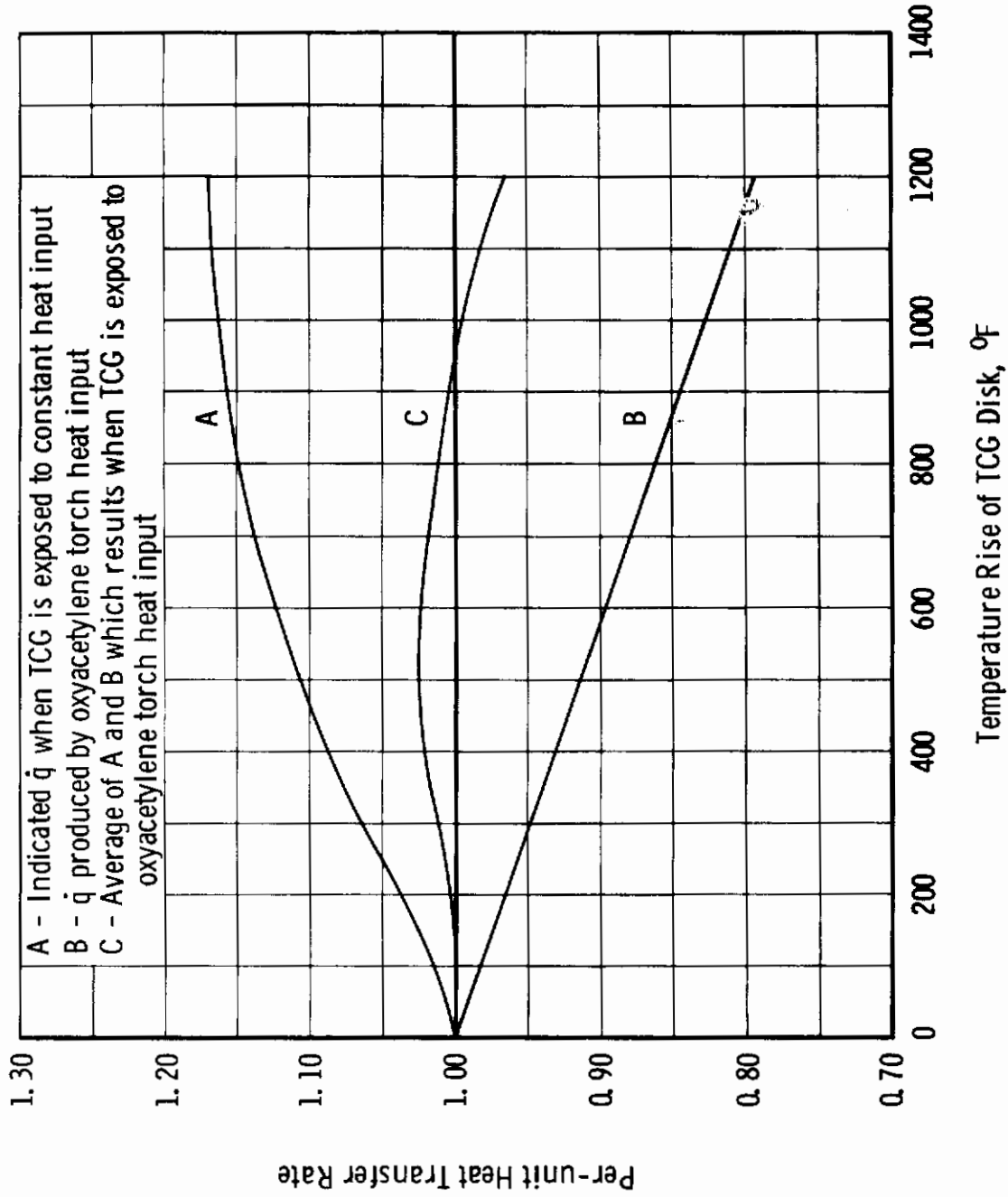


Fig. 4 Heat-Transfer-Rate versus TCG Copper Disk Temperature

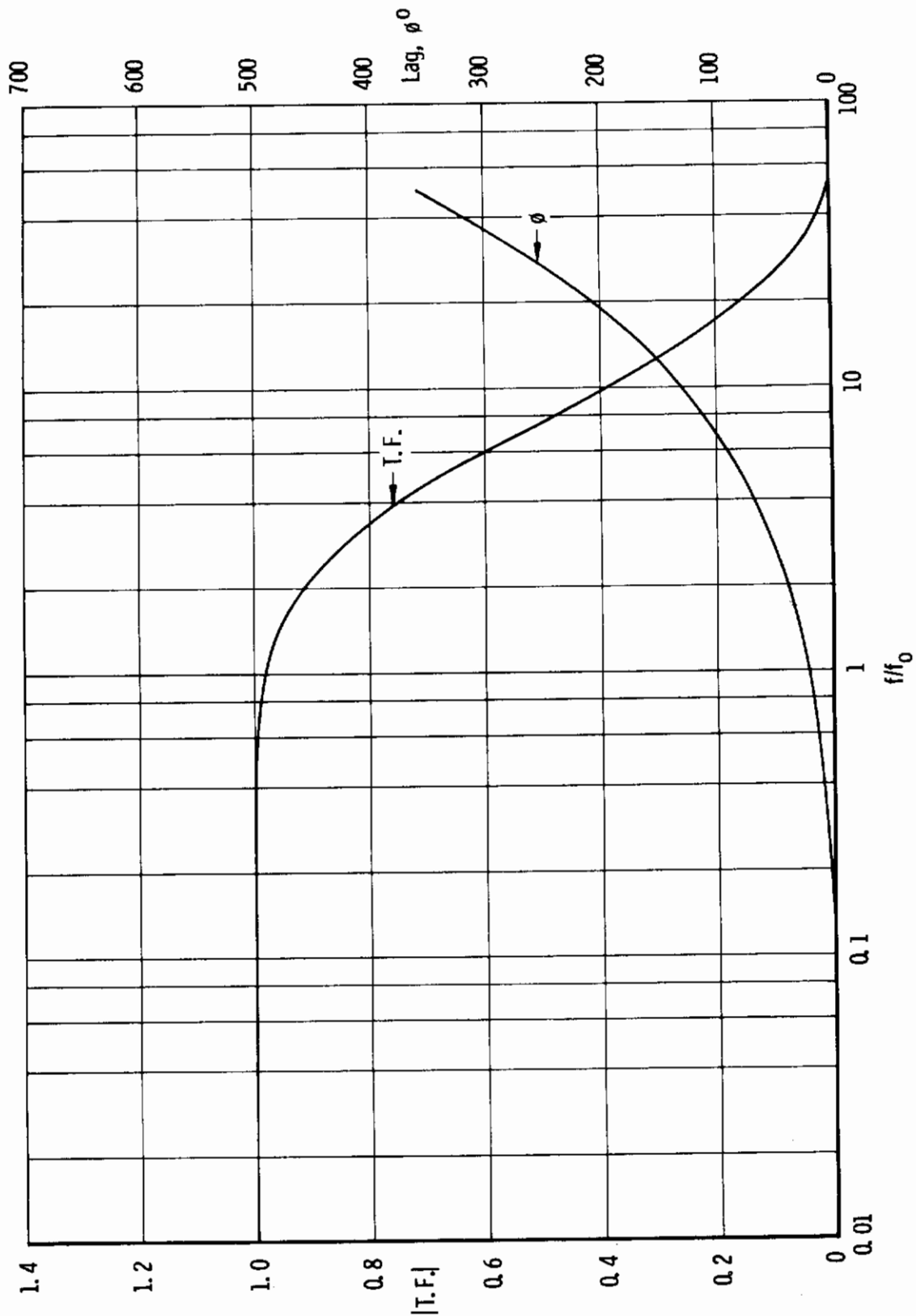


Fig. 5 Transfer Function for a Semi-Infinite Slab

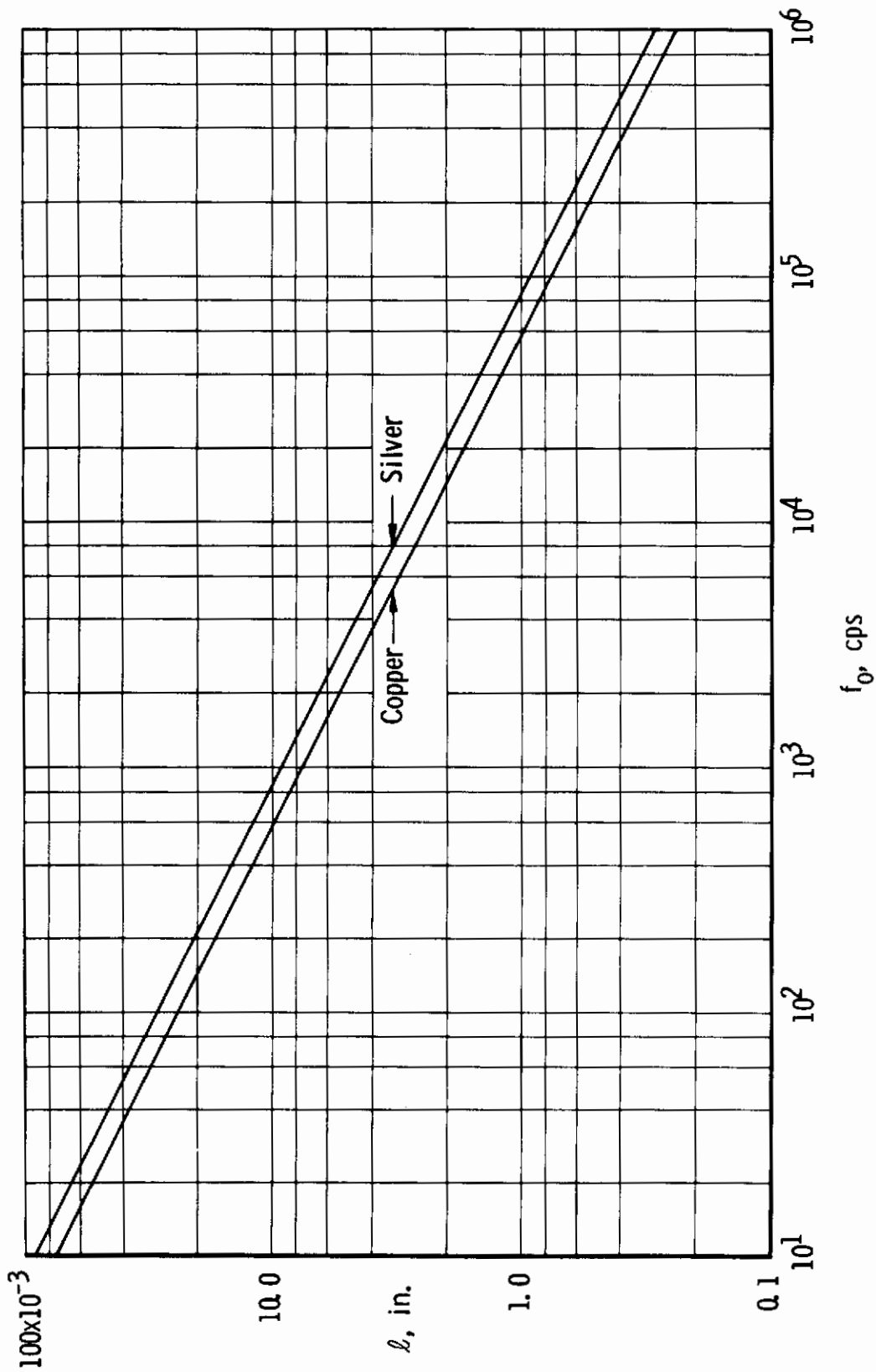


Fig. 6 Slab Thickness versus Frequency

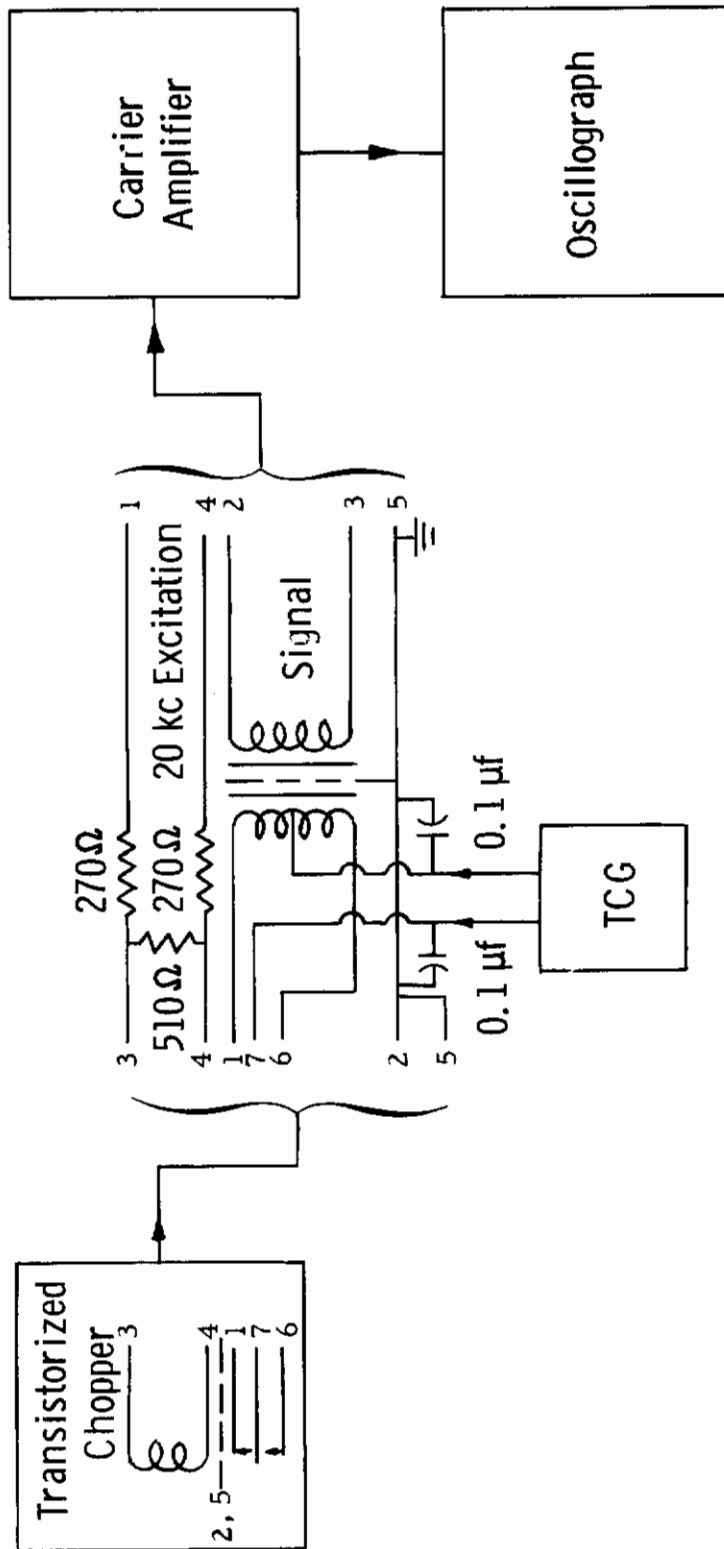


Fig. 7 Instrumentation System for Heat Transfer Measurement with Thermocouple Gage (TCG)

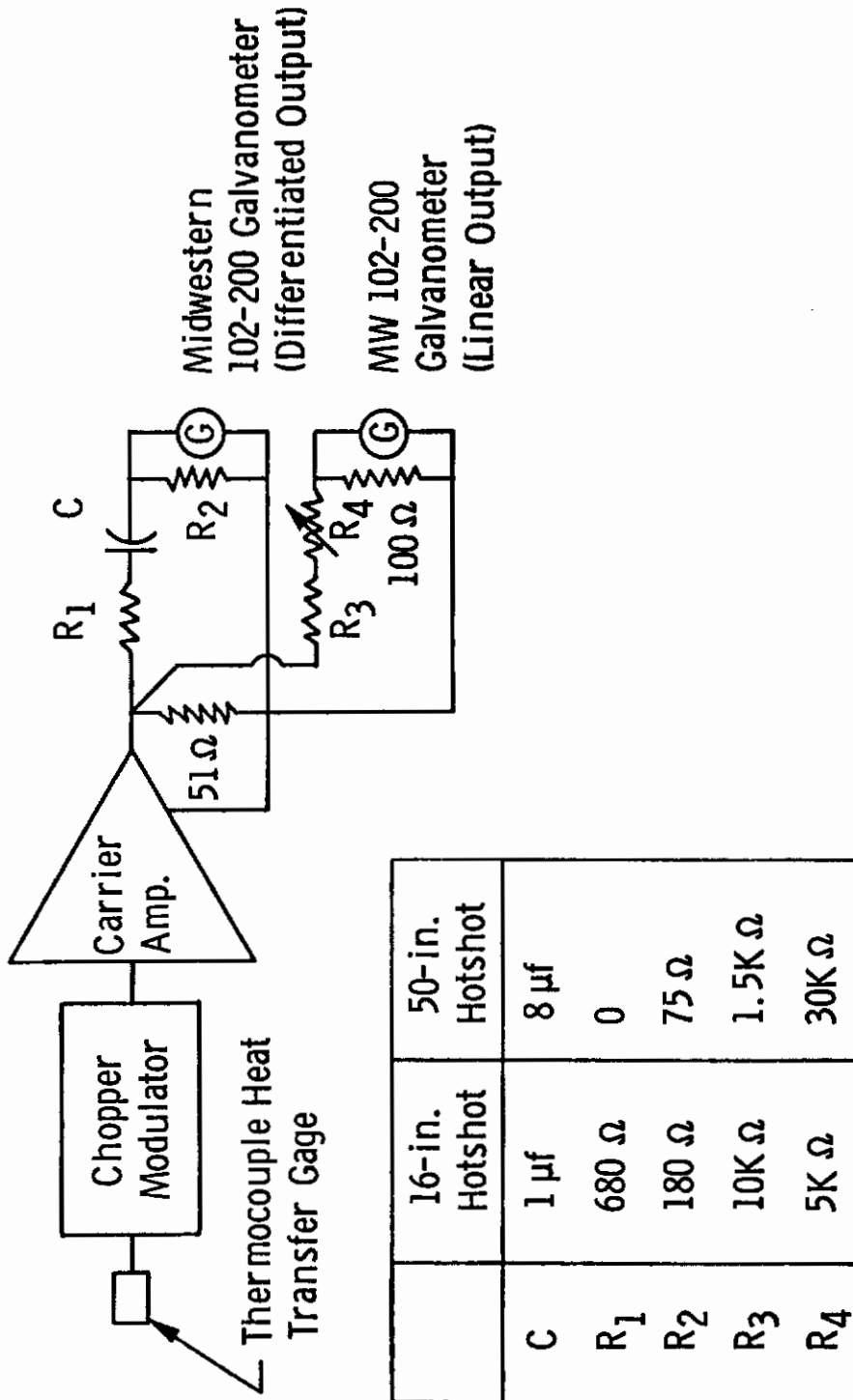


Fig. 8 Heat Transfer Instrumentation System Employing Differentiator

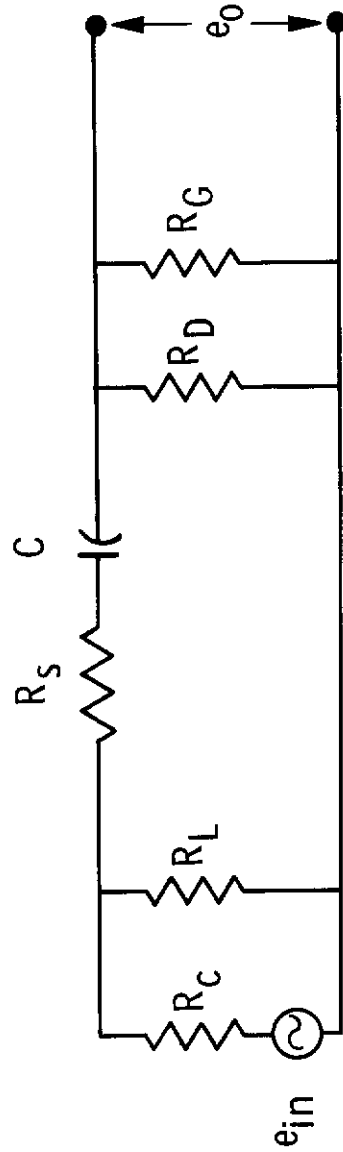


Fig. 9 Differentiator Circuit

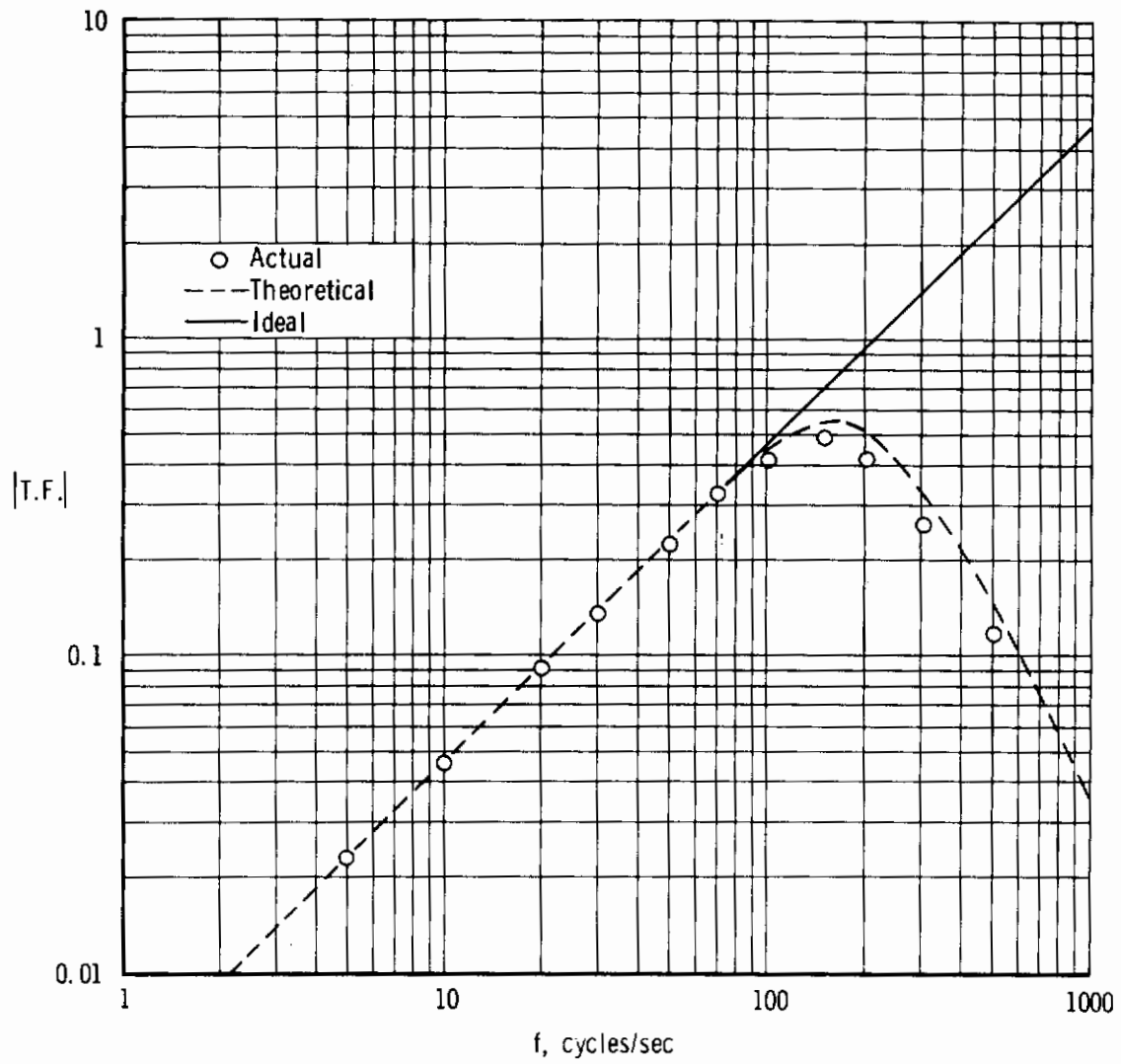


Fig. 10 Transfer Function of Differentiator and Galvanometer

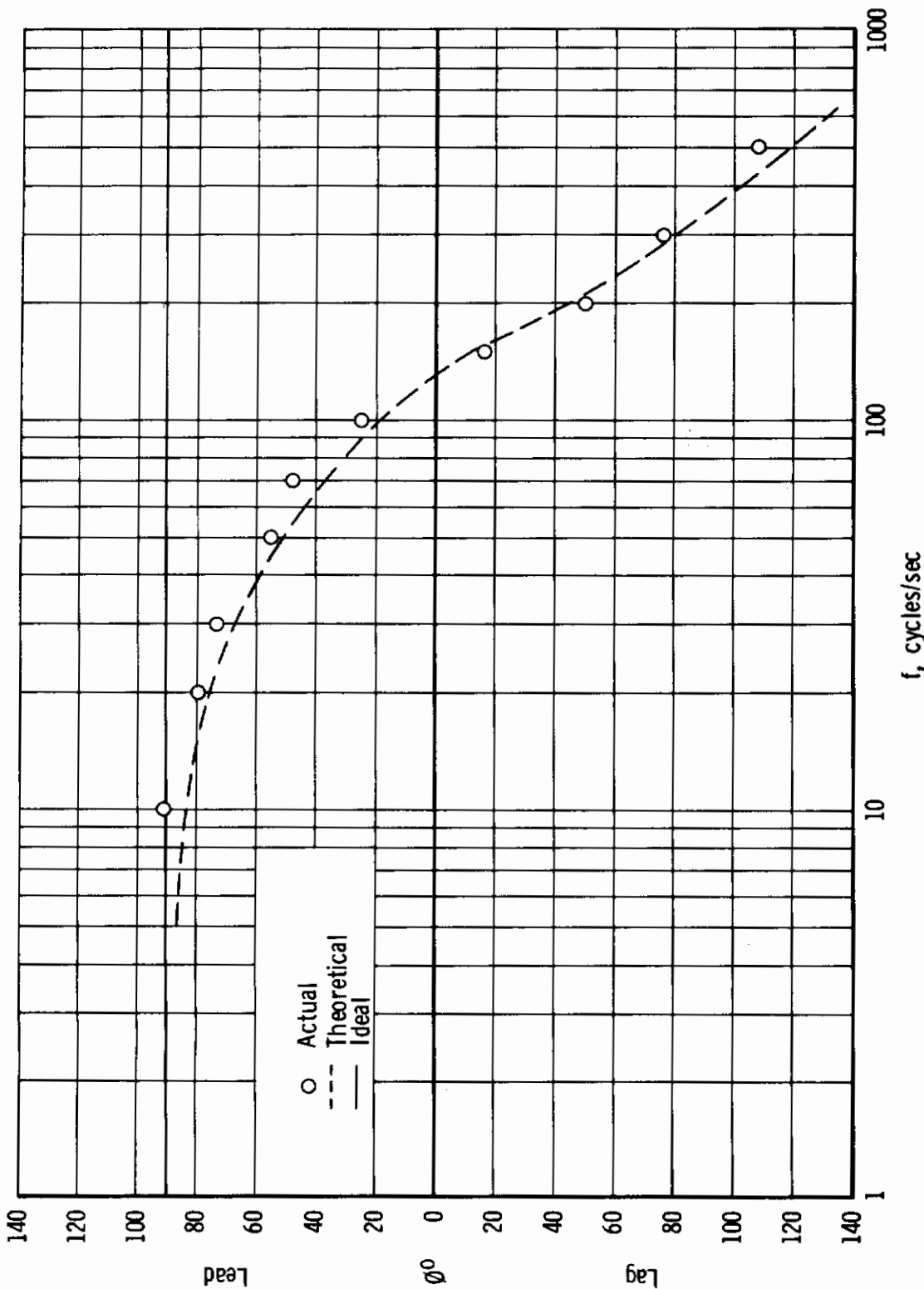


Fig. 11 Phase Shift of Differentiator and Galvanometer

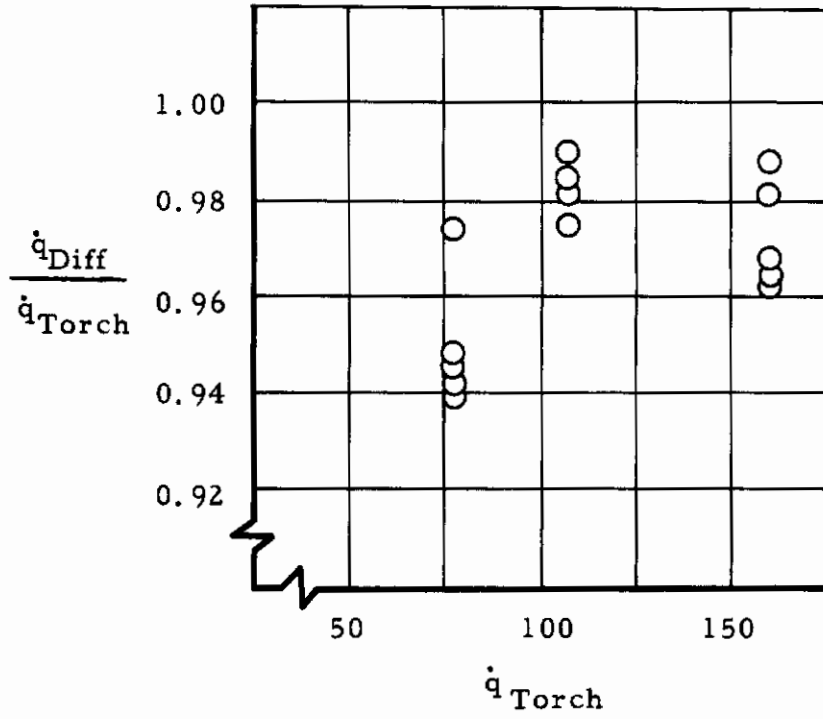


Fig. 12 Comparison of Torch and Differentiator Heat Transfer Data

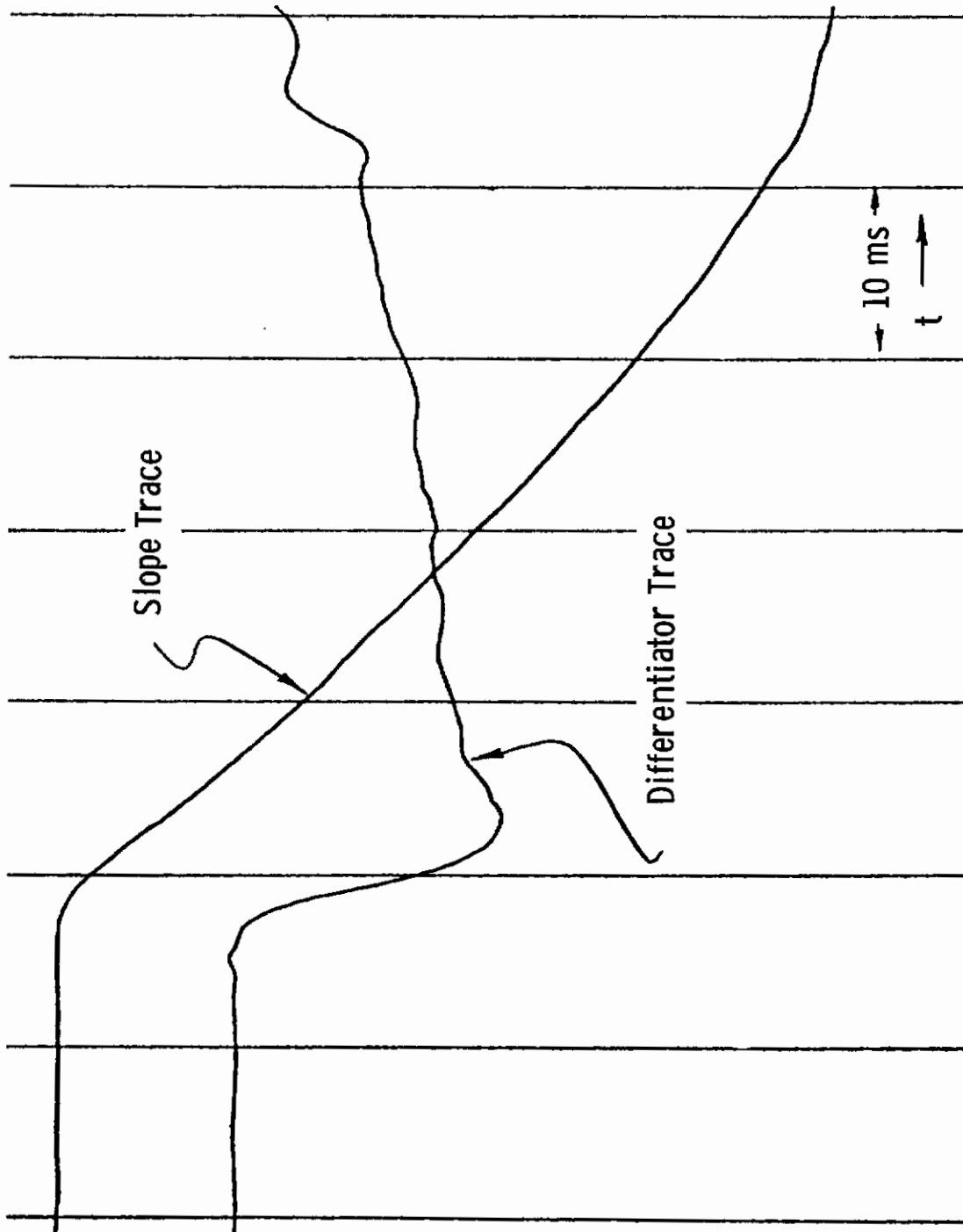
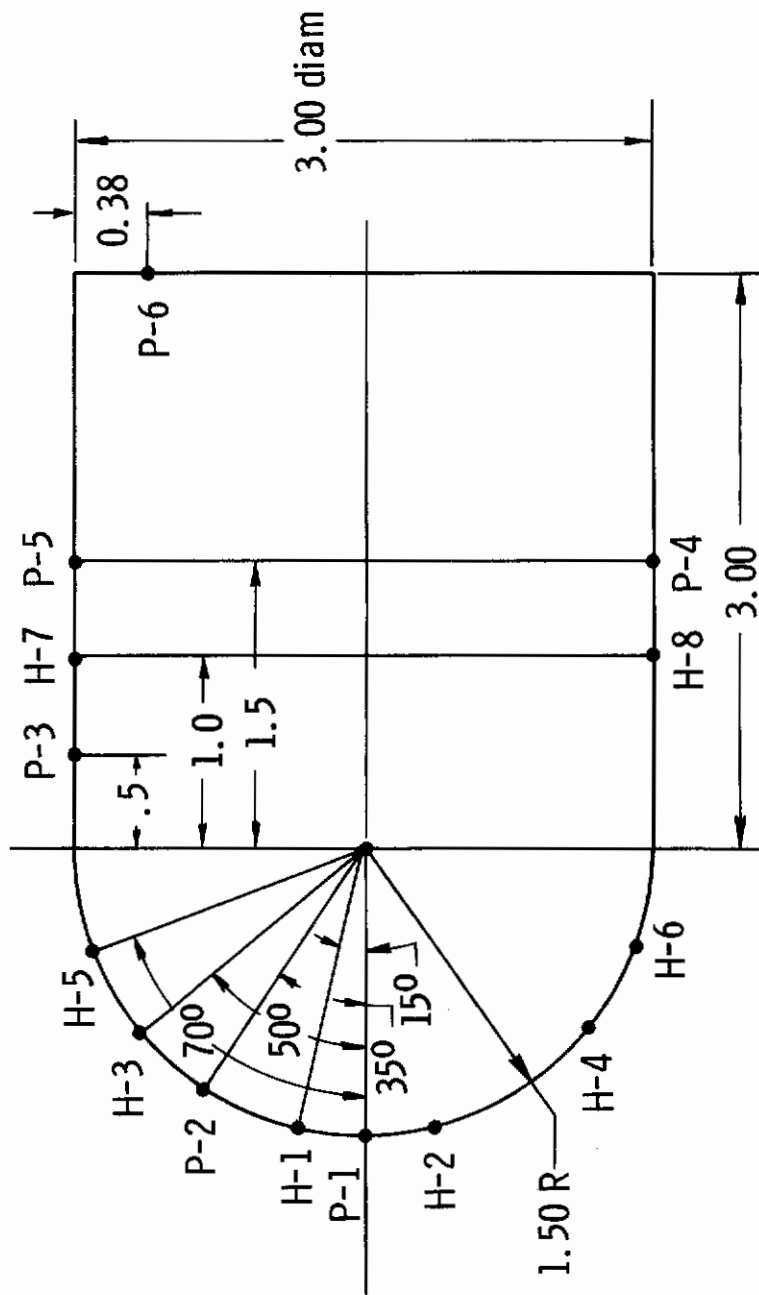


Fig. 13 Typical Oscillographic Trace of Linear and Differentiated TCG Output



P - Pressure
 H - Heat Transfer

Fig. 15 Three-Inch Hemisphere Cylinder Heat Transfer Model

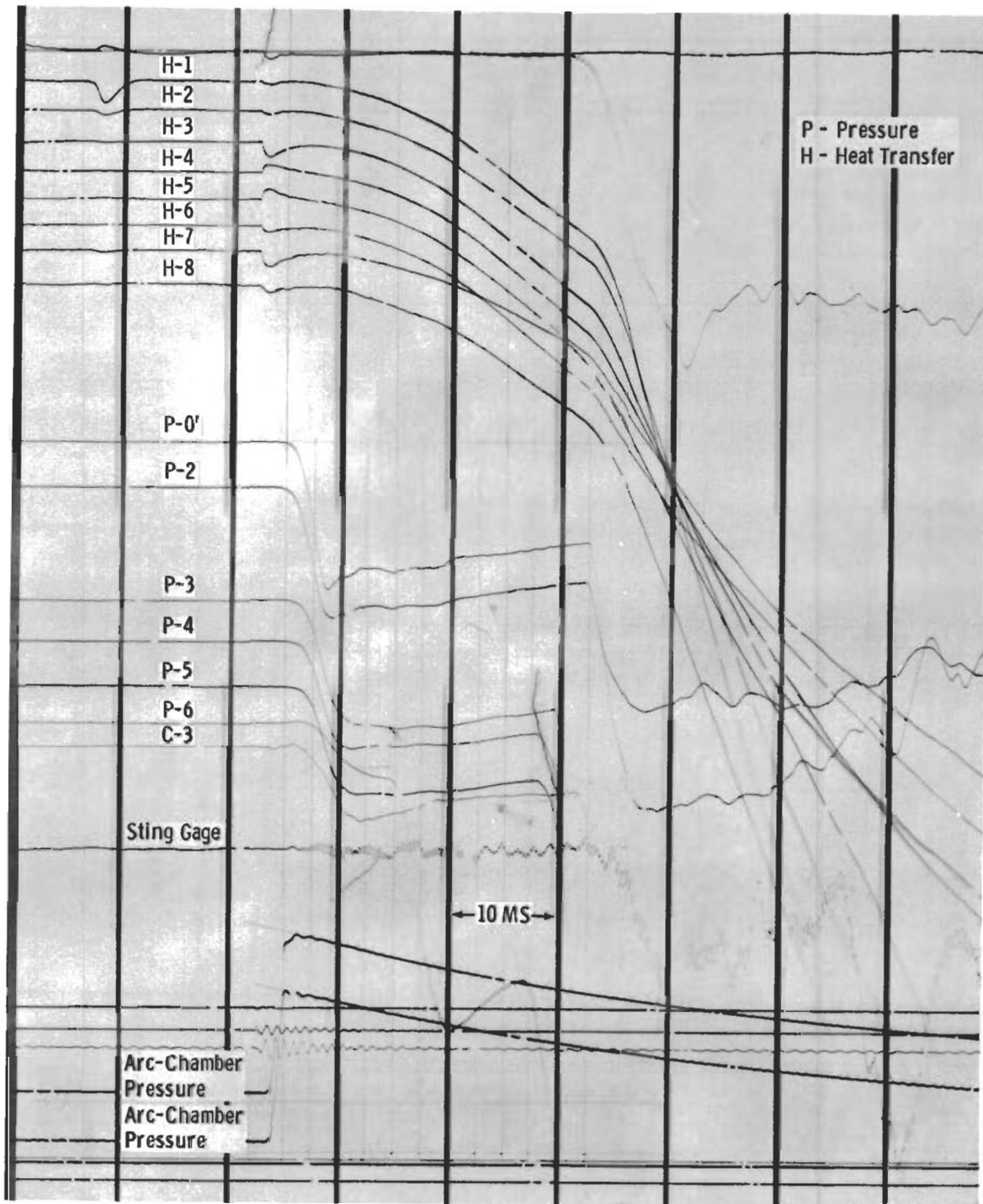


Fig. 16 Hotshot Oscillographic Data Trace

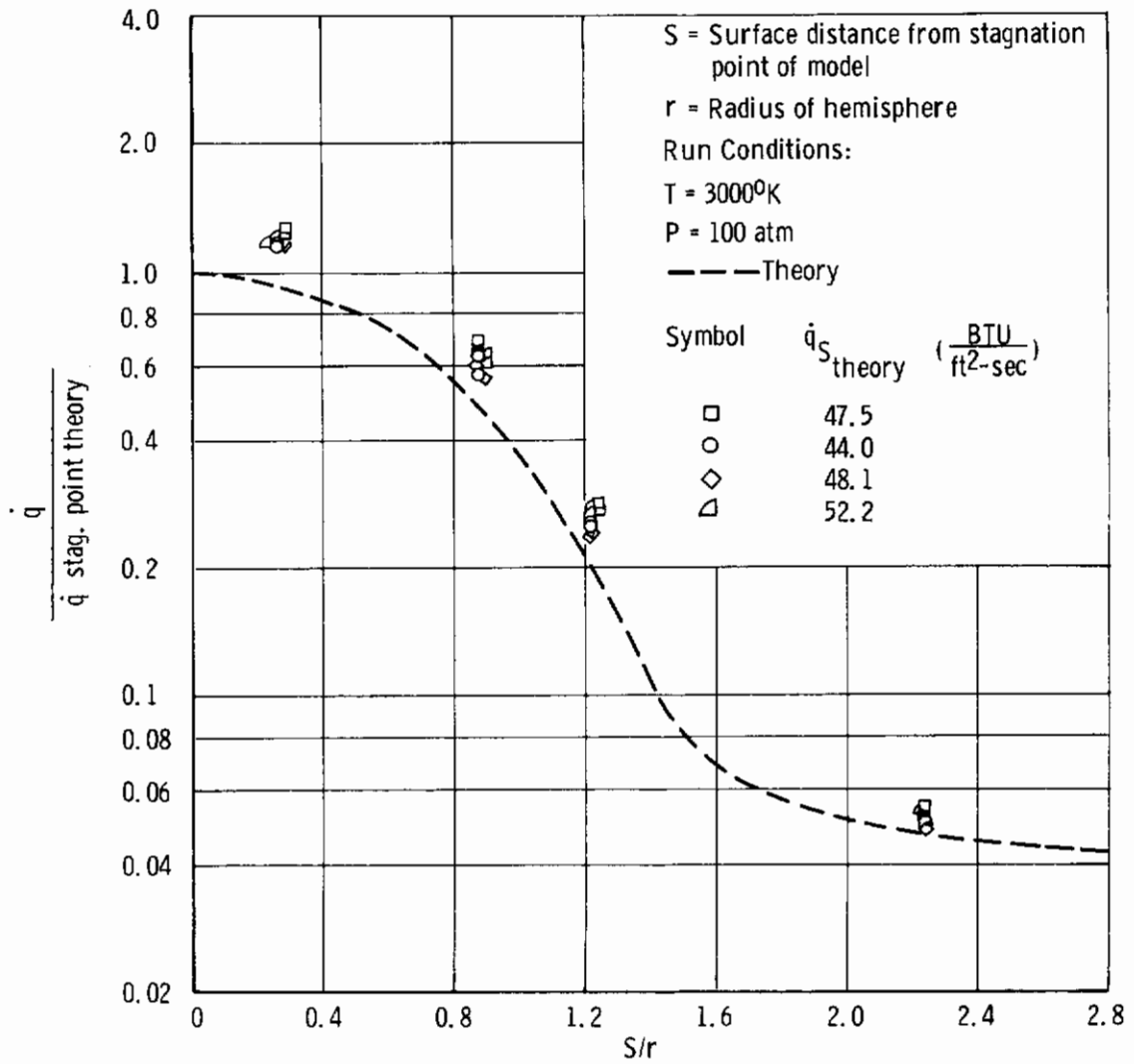


Fig. 17 Comparison between Theoretical and Experimental Heat Transfer Ratio versus S/r